*Protein Science* (1998), 7:293–299. Cambridge University Press. Printed in the USA.
Copyright © 1998 The Protein Society

# Substrate binding and conformational changes of *Clostridium glutamicum* diaminopimelate dehydrogenase revealed by hydrogen/deuterium exchange and electrospray mass spectrometry

FANG WANG,[1] GIOVANNA SCAPIN,[1] JOHN S. BLANCHARD,[1] AND RUTH HOGUE ANGELETTI[2]

[1]Department of Developmental and Molecular Biology, Albert Einstein College of Medicine, Bronx, New York 10461
[2]Department of Biochemistry, Albert Einstein College of Medicine, Bronx, New York 10461

(RECEIVED August 19, 1997; ACCEPTED October 2, 1997)

## Abstract

*C. glutamicum meso*-diaminopimelate dehydrogenase is an enzyme of the L-lysine biosynthetic pathway in bacteria. The binding of NADPH and diaminopimelate to the recombinant, overexpressed enzyme has been analyzed using hydrogen/deuterium exchange and electrospray ionization/mass spectrometry. NADPH binding reduces the extent of deuterium exchange, as does the binding of diaminopimelate. Pepsin digestion of the deuterated enzyme and enzyme–substrate complexes coupled with liquid chromatography/mass spectrometry have allowed the identification of eight peptides whose deuterium exchange slows considerably upon the binding of the substrates. These peptides represent regions known or thought to bind NADPH and diaminopimelate. One of these peptides is located at the interdomain hinge region and is proposed to be exchangeable in the "open," catalytically inactive, conformation but nonexchangeable in the "closed," catalytically active conformation formed after NADPH and diaminopimelate binding and domain closure. Furthermore, the dimerization region has been localized by this method, and this study provides an example of detecting protein–protein interface regions using hydrogen/deuterium exchange and electrospray ionization.

**Keywords:** amide hydrogen exchange; diaminopimelate dehydrogenase; electrospray ionization mass spectrometry; protein conformational change; substrate binding

Isotopic exchange rates of amide hydrogens have been used for many years to provide information about the high-order structure, structural changes, and structural dynamics of proteins (Englander et al., 1979; Woodward et al., 1982). With the advent of electrospray ionization mass spectrometry (ESI-MS) has come the ability to investigate intact protein structures using mass spectrometry. The rates of hydrogen/deuterium (H/D) exchange have been monitored by ESI-MS to study denaturation of bovine ubiquitin and hen lysozyme (Katta & Chait, 1993), to characterize structural perturbations in proteins (Robinson et al., 1994), and to probe conformational heterogeneity and stability of apomyoglobin (Wang & Tang, 1996). These studies on intact proteins, which were carried out in solvents that are compatible with ESI-MS, do not provide high resolution information with regard to specific changes within portions of the protein.

Reprint request to: Ruth H. Angeletti, Department of Developmental & Molecular Biology, Albert Einstein College of Medicine, 1300 Morris Park Ave, Bronx, New York 10461; e-mail: angelett@aecom.yu.edu.

By cleaving a protein with a protease, the isotopic exchange rates within peptide segments defined by protease cleavage can be measured after isolation of the peptides (Rosa & Richards, 1979; Englander et al., 1985; Mallikarachchi et al., 1989). This protein fragmentation method has been recently coupled with on-line liquid chromatography-mass spectrometry (LC-MS) (Zhang & Smith, 1993; Smith et al., 1997). This method has been applied to the study of rabbit muscle aldolase (Zhang et al., 1996), the differences between apo- and holomyoglobin (Johnson & Walsh, 1994), and point mutations of a bacterial phosphocarrier protein (Johnson, 1996). More recently, using a similar method, conformational changes of *E. coli* dihydrodipicolinate reductase induced by substrate and inhibitor binding have been observed. Peptic peptides derived from these complexes, which include the regions of binding sites of the substrate and inhibitor, respectively, have been used to localize these sites. Furthermore, two additional peptides, which are located at the inter-domain hinge region, have also been localized, and are proposed to be exchangeable in the "open," catalytically inactive conformation, but are nonexchangeable in the "closed," catalytically active conformation formed after co-factor and inhibitor binding and domain closure (Wang et al., 1997).

The protein fragmentation/ESI-MS method has now been used to investigate substrate binding and conformational changes of *C. glutamicum meso*-diaminopimelate dehydrogenase (DapDH), an enzyme of the L-lysine biosynthetic pathway in bacteria. *Meso*-diaminopimelate (DAP) is an essential component of the peptidoglycan layer of bacterial cell walls, and disruption of its biosynthesis results in cell death, probably due to instability of the peptidoglycan (Pavelka & Jacobs, 1996). L-Lysine is produced by the enzymatic decarboxylation of *meso*-diaminopimelate and is essential for protein synthesis. Therefore, enzymes of the L-lysine biosynthesis pathway have been investigated as targets for bacterial inhibitor design, and inhibitors developed against enzymes present in this pathway are unlikely to have toxic side effects (Abbot et al., 1994). Three routes are known for biosynthesis of DAP and lysine in bacteria. In the dehydrogenase pathway, the intermediate tetrahydrodipicolinate, common to all three pathways, is converted in a single step to the ultimate lysine precursor, DAP, by a reaction catalyzed by DapDH, as shown in Scheme 1. The gene encoding the *C. glutamicum* enzyme has been sequenced (Ishino et al., 1987) and recently overexpressed in *E. coli*, purified to homogeneity, crystallized (Reddy et al., 1996), and structurally characterized at 2.2 Å resolution (Scapin et al., 1996). The three-dimensional structure of the DapDH–NADP$^+$ complex reveals a three-domain protein: the N-terminal domain is involved in nucleotide binding; the C-terminal domain was proposed to be the site of substrate binding on the basis of the binding of two molecules of acetate bound in this region. In the present investigation, H/D exchange coupled with proteolysis, HPLC and ESI-MS have been used to probe binding of substrates to the recombinant, overexpressed enzyme DapDH and conformational changes of DapDH after substrate binding.

## Results and discussion

The 320-amino acid diaminopimelate dehydrogenase catalyzes the unique, reversible NADP$^+$-dependent oxidative deamination of an amino acid of D configuration (Scheme 1). *C. Glutamicum* DapDH is a homodimer with a molecular weight of 70,399 Da, and is highly specific for DAP ($K_m$ = 3.1 mM) and NADP$^+$ ($K_m$ = 0.13 mM) as substrates (Misono et al., 1986). The three-dimensional crystal structure of the enzyme–NADP$^+$ complex has been determined at 2.2 Å, and a potential DAP binding site was proposed from considerations of stereochemistry, electrostatics, and the binding of two molecules of acetate to this region (Scapin et al., 1996). We have previously shown that ESI-MS, coupled with protease fragmentation and HPLC, can be used to define the substrate binding site using hydrogen/deuterium exchange (Wang et al., 1997). The present study was initiated to confirm the potential of above method, and to define the binding sites for NADPH and DAP to DapDH.

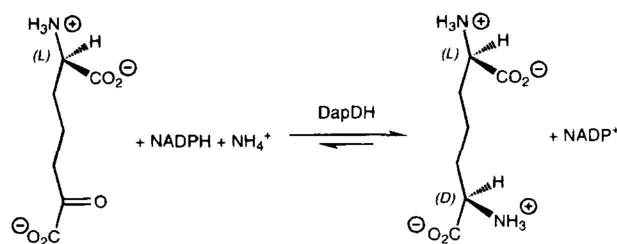

**Scheme 1.** Reaction catalyzed by diaminopimelate dehydrogenase.

### *Global H/D studies*

Global H/D exchange was analyzed for the enzyme in 100 mM sodium cacodylate buffer, pD 6.5, in the presence of either NADPH, DAP, or NADPH and DAP, and the results shown in Figure 1 were obtained. Completely deuterated DapDH was obtained by heating the enzyme in 2 M urea-$d_4$ in 95 atom % excess $D_2O$ for one and half hours at 55 °C, and the completely deuterated DapDH was used as a control to calculate deuterium loss during both pepsin digestion and LC-MS analysis of deuterated DapDH. The extent of H/D exchange into DapDH alone compared to the DapDH–NADPH, DapDH–DAP, and DapDH–NADPH–DAP complexes demonstrates the reduction of exchange rate in the binary and ternary complexes. Deuterium incorporation is reduced ~10% in the DapDH–NADPH and DapDH–DAP binary complexes and ~17% in the DapDH–NADPH–DAP ternary complex (error: <3%), compared to DapDH alone, suggesting that substrate binding is preventing the exchange of either backbone or side-chain hydrogens in these complexes. To localize the regions of DapDH where exchange was inhibited by substrate binding, we repeated these experiments and treated these samples with pepsin to generate peptides that could be individually analyzed and identified according to the known sequence and structure of the enzyme.

### *Identification of peptic peptides*

Pepsin cleaves proteins rather unpredictably, and therefore, peptide mass alone is insufficient for the unambiguous determination of

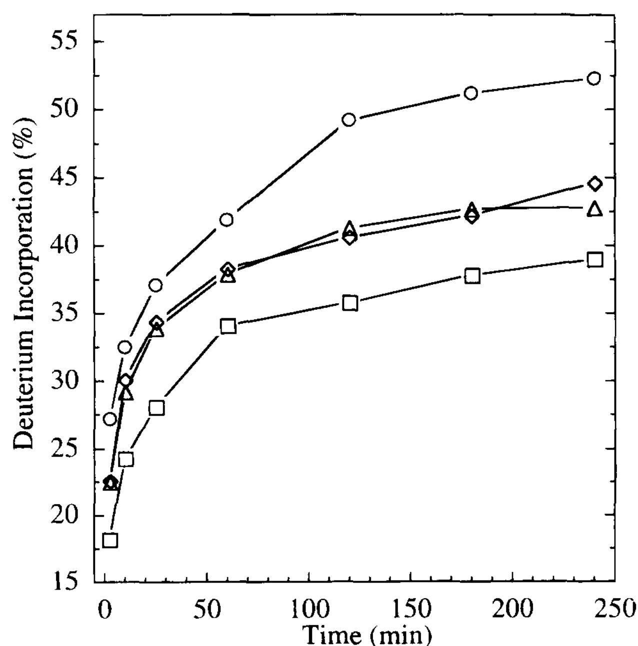

**Fig. 1.** Percentage of deuteriums at peptide amide positions as a function of time in DapDH alone (circles) and in DapDH in the presence of either a 2 mM NADPH (triangles), or 30 mM DAP (diamonds), or 2 mM NADPH and 30 mM DAP (squares).

peptide identification (Wang et al., 1997). An example of this ambiguity, and its resolution, is demonstrated in Figure 2. Eight peptides of molecular mass 2,303 ± 1 could be generated by pepsin hydrolysis of DapDH, corresponding to residues 15–35, 90–109, 124–143, 135–155, 136–156, 162–181, 196–215, and 266–286. The tandem mass spectrum of the HPLC-purified peptide obtained from pepsin digestion of DapDH is shown in Figure 2 and identified as corresponding to residues 136–156. The peptic peptides derived from DapDH by pepsin digestion were separated by HPLC and identified by tandem mass spectrometry (MS/MS). Figure 3 shows the amino acid sequence of *C. glutamicum* DapDH and illustrates the 27 peptides, representing 82% of the total protein sequence, used in this study to identify potential substrate binding regions.

### *Deuterium incorporation within peptide segments*

Most of peptic peptides exhibit essentially identical extents of deuterium exchange in the presence or absence of NADPH or DAP, as shown in Figure 4 for the extent of deuterium incorporation that has occurred after one hour of exchange. Other longer times of exchange points did not reveal any additional differences. Eight peptides are discussed below that show significant differences in the extent of exchange in the presence of NADPH, DAP, or NADPH and DAP.

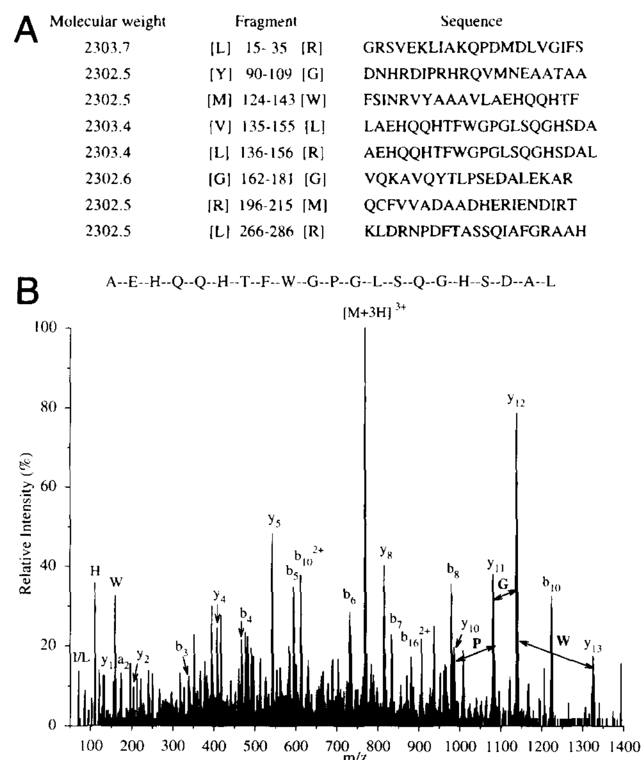

| Molecular weight | Fragment | Sequence |
|---|---|---|
| 2303.7 | [L] 15-35 [R] | GRSVEKLIAKQPDMDLVGIFS |
| 2302.5 | [Y] 90-109 [G] | DNHRDIPRHRQVMNEAATAA |
| 2302.5 | [M] 124-143 [W] | FSINRVYAAAVLAEHQQHTF |
| 2303.4 | [V] 135-155 [L] | LAEHQQHTFWGPGLSQGHSDA |
| 2303.4 | [L] 136-156 [R] | AEHQQHTFWGPGLSQGHSDAL |
| 2302.6 | [G] 162-181 [G] | VQKAVQYTLPSEDALEKAR |
| 2302.5 | [R] 196-215 [M] | QCFVVADAADHERIENDIRT |
| 2302.5 | [L] 266-286 [R] | KLDRNPDFTASSQIAFGRAAH |



**Fig. 2.** An example for the determination of peptide identification. **A:** The list of possible peptides of the molecular weight of 2,303 ± 1. **B:** MS/MS spectrum of the triple protonated peptic peptide ($[M + 3H]^{3+}$) representing residues 136–156 of DapDH. Some of the fragment ions have been labeled according to the nomenclature proposed by Biemann (1988).

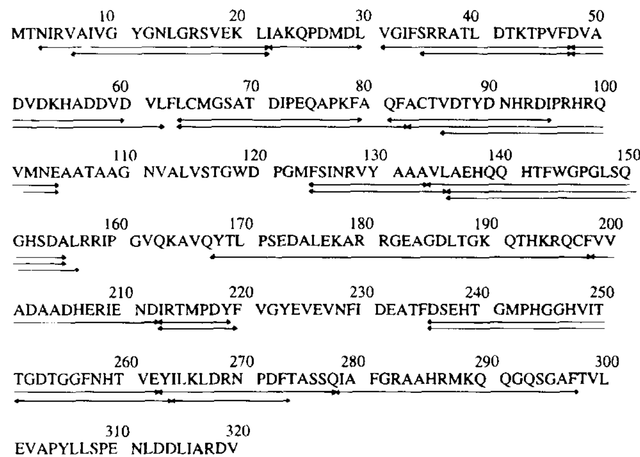


**Fig. 3.** Amino acid sequence of DapDH indicating the position and sequence of peptic peptides evaluated in this study.

### *NADPH binding region*

The peptides representing residues 7–21 and 31–47 show a ~20% decrease in the extent of deuterium exchange in the presence of NADPH (Fig. 5A, B), which is not affected by the additional presence of DAP. Examination of the three-dimensional structure of the DapDH–$NADP^+$ binary complex provides an explanation for above results. Residues 7–21 constitute portions of the first $\beta$-strand and first $\alpha$-helix of the nucleotide binding domain, and residues 31–47 constitute portions of the second $\beta$-strand and the loop between the second $\beta$-strand and the second $\alpha$-helix. The 2′ phosphate of the nucleotide is positioned in a pocket made up of the side-chain atoms of Thr35, Arg36, and Arg37, and the main-chain atoms of Gly10 and Phe11. The pyrophosphate moiety is located directly over the "dinucleotide binding helix" and interacts with main-chain and side-chain atoms of residues of the loop that connects the first $\beta$-strand to the first $\alpha$-helix (Gly12–Gly15). Similar exchange behavior is exhibited by peptides corresponding to residues 48–60 and 83–104 in the amino-terminal nucleotide binding domain, as shown in Figure 4. Residues 48–60 constitute portions of the second $\alpha$-helix and the loops between the second $\beta$-strand and the second $\alpha$-helix and between the second $\alpha$-helix and the third $\beta$-strand. Local conformational changes in residues of Ser35–Arg37 upon binding of dinucleotide may affect the second helix and loops.

### *DAP binding region*

The peptide representing residues 136–156 shows ~20% decrease in the extent of deuterium exchange in the presence of DAP (Fig. 5C). Residues 136–156 constitute portions of the sixth $\beta$-strand and the sixth $\alpha$-helix. The main-chain and side-chain atoms of residues of Thr142–Ser149 and Gln150–Gly151 are located in the previously suggested substrate DAP binding site (Scapin et al., 1996). These data appear to confirm this original suggestion and argue that the loop between the sixth $\beta$-strand and the sixth $\alpha$-helix binds DAP, and that DAP binding at this site inhibits deuterium exchange.

The peptide representing residues 264–273 shows ~13% decrease in the extent of deuterium exchange in the presence of

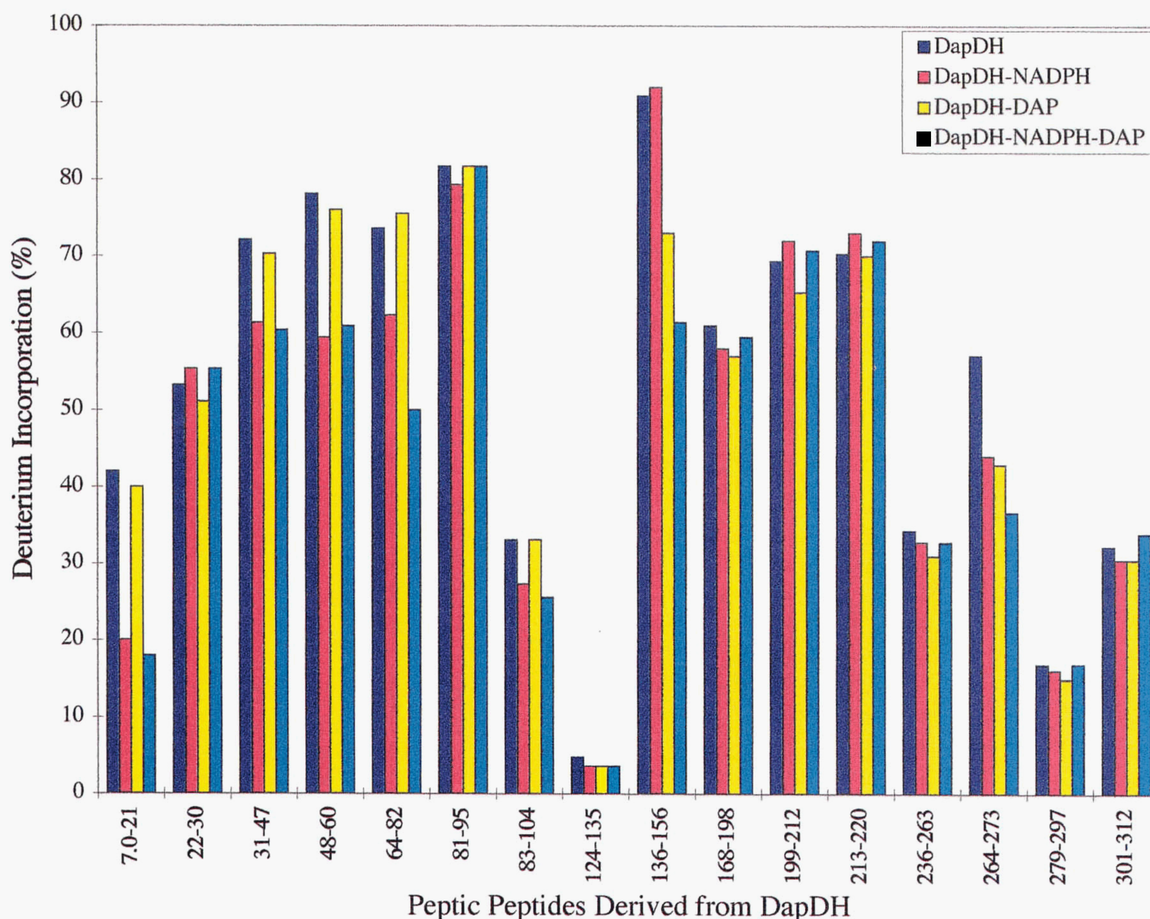


**Fig. 4.** Percentage of deuteriums at peptide amide positions after one hour of deuterium exchange. The typical measurement errors are within 4%.

NADPH or DAP, which decreases ~7% again in the DapDH–NADPH–DAP ternary complex, as shown in Figure 4. The residues of Leu265–Pro271 are located in a region that overlaps the binding sites of both NADPH and DAP.

*Dimerization region*

The peptide representing residues 124–135 shows unusually low deuterium incorporation, as shown in Figure 4. There is ~5% of deuterium incorporation into this region after one hour of deuterium exchange compared to 20–90% incorporation in other peptides. Residues 124–135 constitute the fifth $\alpha$-helix of the dimerization domain, and structurally can be mapped to the interface region between two monomers. This observation of very inhibited exchange may have the potential to probe and identify regions involved in protein–protein interactions.

*A structural model*

Some of these data are graphically presented in Figure 6A, where the peptide fragments whose deuterium exchange are affected by NADPH and/or DAP binding in the structure of the DapDH–NADP$^+$ complex are color coded. Those residues, which appear in peptide fragments that are more slowly exchanged in the presence of NADPH, are shown in dark blue (7–21 and 31–47). Those residues that appear in the peptide fragment that is more slowly exchanged in the presence of DAP are shown in red (136–156). Those residues that appear in the peptide fragment that is more slowly exchanged compared to other peptides are shown in yellow (124–135). Figure 6B is the ribbon diagram of the dimer of DapDH–NADP$^+$ binary complex.

*Hinge movement*

The peptide representing residues 136–156 is also noteworthy because of the effect of added NADPH and DAP on the extent of its exchange (Fig. 5C). The extent of deuterium exchange decreases ~20% in the presence of DAP, and decreases ~10% again in the DapDH–NADPH–DAP ternary complex, but is not affect by the presence of NADPH. The 136–156 peptide includes residues that connect the dimerization domain and the C-terminal domain of the enzyme. The reported structure of the DapDH–NADP$^+$ complex is that of the DapDH dimer. The relative position of the dinucleotide-binding and substrate-binding domain in the two monomers of the dimer are different (Fig. 6B): overlaying the two monomers shows that there is a rigid body movement of the two domains that can be described as a 25° rotation of one region with respect to the other around an ideal axis connecting two interlinkage regions (G145–G147 and H239–G241). This difference in conformation between the two subunits in the crystal structure was due to the presence, in

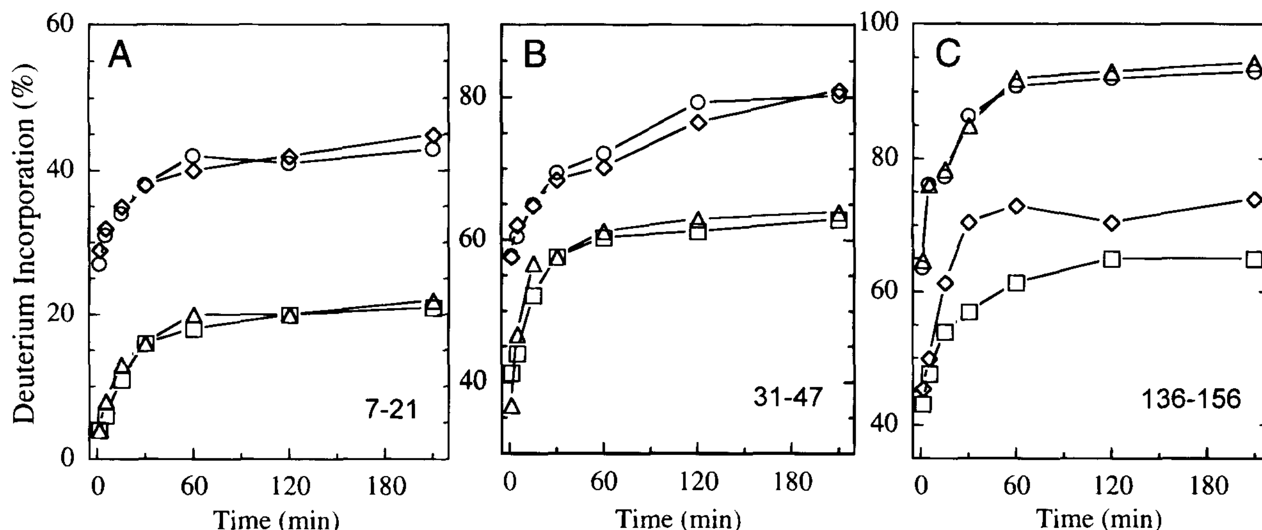


**Fig. 5.** Percentage of deuteriums at peptide amide positions as a function of time in peptides 7–21 (**A**), 31–47 (**B**), and 136–156 (**C**). In all panels, the exchanges have been determined for DapDH alone (circles) or for DapDH in the presence of either a 2 mM NADPH (triangles), or 30 mM diaminopimelate (diamonds), or 2 mM NADPH and 30 mM diaminopimelate (squares).

the closed monomer, of two acetate molecules, that have been proposed to occupy the positions that would have been occupied by the DAP carboxylates (Scapin et al., 1996). The overlay of a DAP molecule onto the two acetate molecules shows that, in the closed monomer conformation, the substrate D-amino acidic center would be positioned about 2.8 Å away from the nicotinamide C4, a reasonable distance for the hydride transfer to occur. In the open form of the enzyme, both the dinucleotide-binding and the substrate-binding area are exposed to the bulk solvent, while in the closed monomer they are surrounded by protein atoms and are solvent inaccessible, with the exception of discrete water molecules in the catalytic site. The open conformation of the monomer represents then the "binding" form of the enzyme, and the closed conformation the "active" form of the dehydrogenase. Binding of NADP(H) alone does not cause the protein to close into the active form; the rigid body movement of the two domains may occur only after binding of substrate. Our data certainly support the original proposal that there is a hinge movement to reorient the C-terminal domain into a catalytically active, "closed" conformation.

The peptide representing residues 64–82 shows ~11% decrease in the extent of deuterium exchange in the presence of NADPH, which is not observed in the presence of DAP, but decreases an additional ~12% in the DapDH–NADPH–DAP ternary complex, as shown in Figure 4. The residues of Cys65–Ser68 are located in the binding region of the adenosyl-ribose of NADPH (Scapin et al., 1996), and the extent of deuterium exchange is lowered upon NADPH binding. The extent of deuterium exchange is further lowered upon the binding of DAP to the DapDH–NADPH binary complex as the residues of Ser68–Asp71 are further shielded from solvent after domain movement leading to the formation of the closed conformation.

### *Kinetic mechanism*

An unusual feature of the exchange patterns observed for the *C. glutamicum* dehydrogenase is the ability of either pyridine nucleotide or *meso*-diaminopimelate to affect hydrogen exchange parameters reflective of conformational changes. The *Bacillus subtilis* diaminopimelate dehydrogenase has been extensively characterized (Misono & Soda, 1980), and the kinetic mechanism for the dehydrogenase from that source has been reported to be ordered, with $NADP^+$ binding preceding *meso*-DAP binding, and with ammonia, L-2-amino-6-oxo-pimelate and NADPH being released in that order. If the *C. glutamicum* dehydrogenase were to exhibit the same ordered kinetic mechanism, then no effect on the hydrogen exchange parameters would be expected to be observed in the presence of *meso*-DAP alone in the absence of $NADP^+$, because binding of *meso*-DAP would only occur to the performed E–$NADP^+$ complex. This is clearly not the case, suggesting that the *C. glutamicum* enzyme may exhibit a random order of addition of substrates. We have previously shown that the *C. glutamicum* diaminopimelate dehydrogenase catalyzes transfer of the pro-R hydrogen of NADPH to the imine formed from the keto acid substrate (Scapin et al., 1996) in contrast to the results reported for the *B. subtilis* enzyme (Misono & Soda, 1980). These differences may extend to the kinetic mechanism exhibited by the two diaminopimelate dehydrogenase. Differences in the kinetic mechanism exhibited by enzymes catalyzing pyridine nucleotide-dependent amino acid oxidation from different sources have been observed (Brunhuber & Blanchard, 1994). Studies are underway to confirm these potential differences in stereochemistry and kinetic mechanism between the *B. subtilis* and *C. glutamicum* *meso*-diaminopimelate dehydrogenases.

## Materials and methods

### *Materials*

Recombinant *C. glutamicum* DapDH was expressed and purified as previously described (Reddy et al., 1996). Pepsin was from the Worthington Biochemical Co. (Freehold, NJ), and $D_2O$ (99.9 atom % D) was from Isotec. Inc. (Miamisburg, OH). All other chemicals and reagents were of the highest grade commercially available.

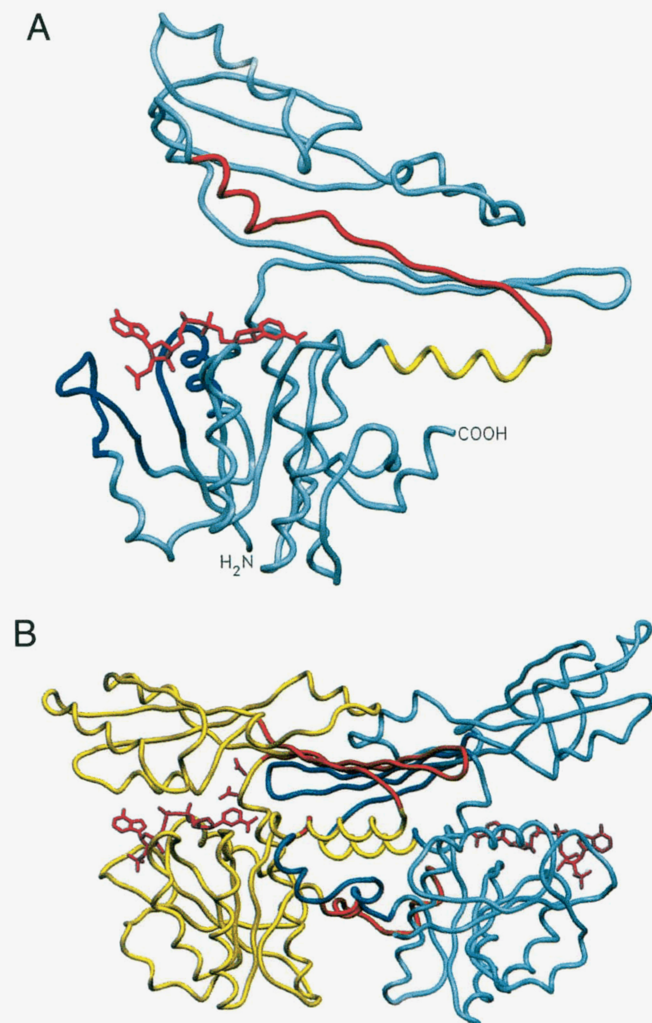


**Fig. 6.** **A:** Ribbon diagram of the three-dimensional structure of one of the monomers of the *C. glutamicum* DapDH–$NADP^+$ binary complex showing the bound $NADP^+$ in cyan. Residues in peptic peptides whose deuterium exchange is lower in the presence of NADPH are shown in dark blue, while residues in the peptic peptide whose deuterium exchange is lower in the presence of DAP are shown in red. Residues in the peptic peptide whose deuterium incorporation is much lower than those in other peptides are shown in yellow. **B:** Ribbon diagram of the dimer of DapDH–$NADP^+$ binary complex showing the bound $NADP^+$ and two acetate molecules in cyan. Monomer 1 is shown in yellow and monomer 2 in blue. The dimerization domains in the monomers are represented with different colors for monomer 1 and 2: orange for monomer 1 and blue for monomer 2. Residues 124 through 135 are yellow in both monomers.

### *Exchange studies*

H/D exchange was initiated by dilution of 5 $\mu$L of a 700 $\mu$M solution of DapDH in 100 mM sodium cacodylate buffer, pH 6.5, in the presence or absence of 2 mM NADPH or/and 30 mM DAP, into 95 $\mu$L of corresponding deuterated buffer in 99 atom % excess $D_2O$, in the presence or absence of 2 mM NADPH or/and 30 mM DAP. Solutions were maintained at room temperature, and allowed to exchange for various lengths of time. At appropriate intervals, aliquots of the DapDH solution were adjusted to pH 2.2 by the addition of an equal volume of the quench solution (0.5 M ammonium phosphate, pH 2.2), and immediately cooled to 0 °C to be subject to either LC-ESI-MS analysis or peptic digestion and subsequent LC-ESI-MS analysis, to determine the extent of deuterium incorporation into DapDH or the peptic peptides.

### *Pepsin digestion*

Exchanged solutions of DapDH were quenched and digested by adding equal volume of 0.5 M ammonium phosphate buffer, pH 2.2, containing 17.5 $\mu$M pepsin, and incubated for 2 min at 0 °C.

### *LC-ESI-MS analysis of the deuterated DapDH and its peptic peptides*

LC-ESI-MS analysis of deuterated DapDH and its peptic peptides were performed to determine the extent of deuterium incorporation into DapDH and different regions of DapDH. A Shimadzu HPLC equipped with two LC-10AD pumps was used to pump the solvents at 50 $\mu$L/min and to generate acetonitrile gradients. Solvent A is $H_2O$ containing 0.05% trifluoroacetic acid (pH 2.2) and solvent B is 90% acetonitrile containing 10% $H_2O$ and 0.05% trifluoroacetic acid. The Rheodyne injector, column, and transfer line were immersed in an ice bath (0 °C) to minimize back exchange with HPLC solvents. Aliquots (50 $\mu$L) of the exchanged and quenched protein solution or the peptic digests were loaded onto a Vydac 1.0 × 150 mm $C_4$ or 1.0 × 250 mm $C_8$ column, respectively. After desalting using a 5-min 5–10% B gradient, the protein eluted at ~12 min with a 2-min 10–100% B gradient. The peptic peptides eluted between 11 and 14 min with a 10-min 10–60% B gradient after desalting using a 2-min 5–10% B gradient. The column effluent (50 $\mu$L/min) was delivered directly to the mass spectrometer without flow split. The mass resolution of the spectrometer was tuned to give a constant peak width of 1 Da (full width at half maximum) across the mass range of interest. Full scan mass spectra were acquired using a step size of 0.1 Da with a scan time of 3.15 s across the mass range of 830–1400 for the protein sample, and with a scan time of 3.64 s across the mass range of 320–1355 for the peptic digests.

The percentage of deuterium in peptide amide positions in DapDH or DapDH-derived peptic peptides was determined from the mass difference between non-deuterated and deuterated samples after correction for the loss of deuterium during LC-ESI-MS analysis or peptic digestion and subsequent LC-ESI-MS analysis (Zhang & Smith, 1993). Equation 1 is used for the calculation of the percentage of deuterium incorporation,

$$\%D = (m_t - m_0)/(m_{100} - m_0) \times 100 \quad (1)$$

where $m_t$ is the protein (peptide) mass at time $t$, $m_0$ is the protein mass at time zero, and $m_{100}$ is the protein mass at infinite time (completely exchanged). All of the masses used in Equation 1 are experimental masses measured by LC-ESI-MS. Completely deuterated DapDH was obtained by incubating DapDH in 2 M urea-$d_4$ at 55 °C for $1\frac{1}{2}$ h. The fully exchanged DapDH was digested with pepsin, and the back exchange of peptic peptides in this study was determined from the theoretical mass for the completely amide-deuterated fragment and the experimental mass determined after LC-ESI-MS analysis. For the peptic peptides we studied in this paper, the extent of back exchange varies between 25 and 55% during peptic digestion and LC-ESI-MS analysis, consistent with

40–50% of overall back exchange reported by other authors (Johnson & Walsh, 1994; Johnson, 1996).

*Mass spectrometry and tandem mass spectrometry*

All mass spectra were acquired using an API-III triple quadrupole mass spectrometer equipped with an atmospheric pressure ionization (API) source and a pneumatically assisted electrospray interface (PE-SCIEX, Thornhill, Ontario, Canada). High purity nitrogen was used as the nebulizing gas to prevent back exchange of deuterium by laboratory air during the ionspray process. A Macintosh Quadra 950 was used for instrument control, data acquisition, and processing. Tandem mass spectrometry was performed to identify peptic peptides. Fragment ion (tandem) mass spectra were obtained using collision-induced dissociation of precursor ions selected by their $m/z$ value in the first quadrupole. Collisional activation was accomplished by introducing argon into the second (rf-only) quadrupole, and the resulting fragment ions were analyzed in the third quadrupole. Optimum collision conditions varied with the precursor peptides, with target gas thickness ranging from $1.5\text{–}4 \times 10^{14}$ molecules/cm$^2$ and accelerating potential differences into the collision cell in the range of 20–80 eV.

## Acknowledgments

This work was supported by NIH Grant AI 33696 (J.S.B.) and a grant from the Mathers Foundation (R.H.A.). The purchase of the mass spectrometer used in this work was partially supported by a grant from the NIH (RR09113).

## References

Abbot SD, Lane-Bell P, Sidhu KPS, Vederas JC. 1994. Synthesis and testing of heterocyclic analogues of diaminopimelic acid (DAP) and inhibitors of DAP dehydrogenase and DAP epimerase. *J Am Chem Soc 116*:6513–6520.

Biemann K. 1988. Contributions of mass spectrometry to peptide and protein structure. *Biomed Environ Mass Spectrom 16*:99–111.

Brunhuber NM, Blanchard JS. 1994. The biochemistry and enzymology of amino acid dehydrogenases. *Crit Rev Biochem Mol Biol 29*:415–467.

Englander JJ, Rogero JR, Englander SW. 1979. Measurement and calibration of peptide group hydrogen-deuterium exchange by ultraviolet spectrophotometry. *Anal Biochem 92*:517–524.

Englander JJ, Rogero JR, Englander SW. 1985. Protein hydrogen exchange studied by the fragment separation method. *Anal Biochem 147*:234–244.

Ishino S, Mizukami T, Yamaguchi K, Katsumata R, Araki K. 1987. Nucleotide sequence of the *meso*-diaminopimelate D-dehydrogenase gene from *Corynebacterium glutamicum*. *Nucleic Acids Res 15*:3917.

Johnson RS. 1996. Mass spectrometric measurement of changes in protein hydrogen exchange rates that result from point mutations. *J Am Soc Mass Spectrom 7*:515–521.

Johnson RS, Walsh KA. 1994. Mass spectrometric measurement of protein amide hydrogen exchange rates of apo- and holo-myoglobin. *Protein Sci 3*:2411–2418.

Katta V, Chait BT. 1993. Hydrogen/deuterium exchange electrospray ionization mass spectrometry: A method for probing protein conformational changes in solution. *J Am Chem Soc 115*:6317–6321.

Mallikarachchi D, Burz D, Allewell NM. 1989. Effects of ATP and CTP on the conformation of the regulatory subunit of *Escherichia coli* aspartate transcarbamylase in solution: A medium-resolution hydrogen exchange study. *Biochemistry 28*:5386–5391.

Misono H, Ogasawara M, Nagasaki S. 1986. Characterization of *meso*-diaminopimelate dehydrogenase from *Corynebacterium glutamicum* and its distribution in bacteria. *Agric Biol Chem 50*:2729–2734.

Misono H, Soda K. 1980. Properties of meso-alpha, epsilon-diaminopimelate D-dehydrogenase from *Bacillus sphaericus*. *J Biol Chem 255*:10599–10605.

Pavelka MS Jr, Jacobs AR Jr. 1996. Biosynthesis of diaminopimelate, the precursor of lysine and a component of peptidoglycan, is an essential function of *Mycobacterium smegmatis*. *J Bacteriol 178*:6496–6507.

Reddy SG, Scapin G, Blanchard JS. 1996. Expression, purification, and crystallization of meso-diaminopimelate dehydrogenase from *Corynebacterium glutamicum*. *Proteins Struct Funct Genet 25*:514–516.

Robinson CV, Gross M, Eyles SJ, Ewbank JJ, Mayhew M, Hartl FU, Dobson CM, Radford SE. 1994. Conformation of GroEL-bound α-lactalbumin probed by mass spectrometry. *Nature 372*:646–651.

Rosa JJ, Richards FM. 1979. An experimental procedure for increasing the structural resolution of chemical hydrogen-exchange measurements on proteins: Application to ribonuclease S peptide. *J Mol Biol 133*:399–416.

Scapin G, Reddy SG, Blanchard, JS. 1996. Three-dimensional structure of *meso*-diaminopimelic acid dehydrogenase from *Corynebacterium glutamicum*. *Biochemistry 35*:13540–13551.

Smith DL, Deng Y, Zhang Z. 1997. Probing the non-covalent structure of proteins by amide hydrogen exchange and mass spectrometry. *J Mass Spectrom 32*:135–146.

Wang F, Blanchard JS, Tang Xj. 1997. Amide hydrogen exchange/electrospray ionization mass spectrometry studies of substrate and inhibitor binding and conformational changes of *E. coli* dihydrodipicolinate reductase. *Biochemistry 36*:3755–3759.

Wang F, Tang Xj. 1996. Conformational heterogeneity and stability of apomyoglobin studied by hydrogen/deuterium exchange and electrospray ionization mass spectrometry. *Biochemistry 35*:4069–4078.

Woodward C, Simon I, Tuchsen E. 1982. Hydrogen exchange and the dynamic structure of proteins. *Mol Cell Biochem 48*:135–160.

Zhang Z, Post CB, Smith DL. 1996. Amide hydrogen exchange determined by mass spectrometry: Application to rabbit muscle aldolase. *Biochemistry 35*:779–791.

Zhang Z, Smith DL. 1993. Determination of amide hydrogen exchange by mass spectrometry: A new tool for protein structure elucidation. *Protein Sci 2*:522–531.